



Structural
Geology -
Tectonics -
Geomechanics

RWTHAACHEN
UNIVERSITY

Report to Nedmag Industries Mining & Manufacturing B.V.

Billitonweg 1 - 9640 AE Veendam - The Netherlands

Squeeze mining- induced stress changes

in the faulted overburden of the

Veendam salt Pillow

Structural Geology, Tectonics and Geomechanics

RWTH Aachen University, Lochnerstrasse 4-20

D-52056 Aachen, Germany

T:

M:

e-mail:

www.ged.rwth-aachen.de

Aachen, 25.05.2017

Summary

The aim of this work was to quantify the stress development in the faulted overburden of the Veendam Salt pillow, induced by squeeze mining in a salt cavern field, and to evaluate those changes regarding the mechanical stability of the faulted overburden.

Faults in the overburden were mapped in a 3D seismic dataset, and shown to be normal faults with N-S and NE-SW strikes. None of the faults can be shown to continue to the surface, in agreement with the absence of neotectonic activity in the area.

A Finite Element model was used to calculate the stress changes in the Veendam Salt Pillow and its overburden, caused by squeeze mining. We built a model with radial symmetry, and let it develop a geologically stable in-situ stress field as a starting point for the squeeze mining simulations. Using reasonable values of the input geometry and the material properties, the model was ran until about 60 cm of subsidence in 50 years above a 2.4 km wide cavern field.

In most of the overburden, stress changes correspond to reduction of the shear stress and thus mechanically more stable conditions, in agreement with earlier simulations. In a limited volume of the overburden, shear stresses increase, but this increase is small and the stress path is likely to be far from the Mohr-Coulomb failure criterion for fault reactivation. The calculated stress changes are therefore very unlikely to lead to reactivation of the faults in the overburden.

Method - geomechanical modelling

The geomechanical modelling approach used in this study is similar to that of Fokker et al., 1995. To simulate the stress changes in the Veendam Salt Pillow and its overburden, caused by squeeze mining of a cavern field, the Finite Element Method (FEM) software 3DS Abaqus was used. Abaqus is widely used for engineering and material science applications and sets a benchmarked industry standard (<http://www.3ds.com/>).

Results were evaluated considering a Mohr-Coulomb criterion for the brittle overburden. If this criterion is reached in a point where there is a pre-existing fault which is conservatively assumed to be cohesionless and optimally oriented for slip, it is considered to correspond to reactivation of the fault. Here we note that a reactivated fault may or may not move seismically.

The model was calculated in four steps. In the first stage a geostatic stress is established which is followed by a second 3.15×10^{11} s (10,000 years) long step to let the model equilibrate the stress field in the gravity field. In the third phase the pressure in the cavern field is lowered to finally produce about 50 cm or 60 cm of maximal subsidence. Here we report the stress development during cavern convergence in the third model step. In the fourth step abandonment was simulated by keeping the cavern pressure lithostatic for a long period. These results are not discussed here.

FE model setup

The Veendam Pillow has an elliptical shape striking NE-SW and an average diameter of about 10 km (**Fig. 1**). It is surrounded by salt withdrawal basins and other salt structures (i.e. pillows or diapirs) further away. The Veendam and Tripscompagnie cavern field is located around the crest of the eastern part of the pillow. The 13 wells are distributed within an area with a diameter of 2590 m (**Fig. 1**) inside the Zechstein-III 1b to 3b K-Mg salt layers, with an irregular and not well understood shape.

The calculated model is axisymmetric and centered in the middle of the salt pillow and the cavern field **Fig. 2**. This is a simplification to allow axisymmetric modeling which is computationally much less expensive, while preserving the essential mechanical elements of the system. The salt pillow is 10 km in diameter and is 600 m high. The central pillow is surrounded by a ring of thicker salt, representing the salt highs surrounding the Veendam Pillow.

The solution mining field in this model is represented by three ring-shaped caverns with a radius of 220, 670 and 1170 m around the center. The rings are each 100 m high and 150 m wide with rounded edges and located in the center of the K-Mg salt layer (**Fig. 2**). With this ring geometry, the deformation around the caverns is distributed over the whole cavern field while local effects of squeeze between caverns can still be resolved.

Layers

To model the mechanical response of the overburden to squeeze mining, the model was subdivided into several units with different rheologies and mechanical properties (Fokker, 1995; Fokker and Visser, 2014) (**Fig. 2, Table 1**). The Rotliegend subsalt layer is assumed flat, overlain by Zechstein salt. Inside the Zechstein halite unit one K-Mg salt layer is present to represent the softer ZIII 1b to 3b layers. The suprasalt sediments are simplified to a Triassic unit overlain by the Lower and Upper Cretaceous and the Tertiary - Quaternary sediments of the Upper North Sea Supergroup. These units are thicker in the basins than above the pillow center. While the rheology of the salt includes elastic and power law creep behavior (Table

1), the overburden is modeled as elastic: since the aim of this study is to clarify if the overburden stresses during elastic deformation can reach the Mohr Coulomb plasticity criterion, there is no need to include plasticity in the overburden.

Salt rheology

Under the conditions of squeeze mining, evaporites deform elastically and by creep, without dilatancy (et al., 2008). The plastic deformation of evaporites is described by (power law) dislocation creep and (linear) fluid assisted pressure solution / precipitation (PS) creep. Since squeeze mining leads to a geologically rapid deformation, we decided to use power law creep only (Urai et al., 2008). We infer that including the PS creep, while possible, will not significantly change the conclusions relevant to this report.

The rheology of the mixed potassium and magnesium (K-Mg) salts in the 1b layer was chosen to have the same stress exponent as Halite, but about 10 times weaker than rock salt, to simulate a package of Carnallite, Halite and Bischofite (Table 1, et al., 1981; , 1983). Again, this is a strong simplification, but considering that the stress changes in the overburden occur at a distance from the 1b layer which is more than 10x the thickness of typical Bischofite layers, we infer that this will not significantly change the conclusions relevant to this report.

Table 1:

Name	Depth in pillow center [m]	Depth in the basins [m]	Density [Kg/m ³]	Young's Modulus [GPa]	Poisson's Ratio	Creep Multiplier	Creep Exponent
Quaternary + Tertiary	0 to 400	0 to 800	2000	0.25	0.38	-	-
Upper Cretaceous	400 to 900	800 to 1400	2300	10	0.18	-	-
Lower Cretaceous	900 to 1000	1400 to 1500	2350	15	0.23	-	-
Triassic	1000 to 1400	1500 to 2100	2450	10	0.3	-	-
Halite	1400 to 3300	2100 to 3300	2040	30	0.25	1e-44	5
K-Mg salt	1560 to 1630	2230 to 2260	2040	30	0.25	1e-43	5
Rotliegend	3300 to 5000	3300 to 5000	2600	15	0.18	-	-

Model Results

Initial stress

Stresses in the models were computed as total stresses, assuming drained hydrostatic pore pressure everywhere. For stability analyses, effective stresses were computed, using hydrostatic pore pressure. **Figure 3** shows the trend of the minimum and maximum principle stresses in the model. Note that the stress contours in the starting model are not horizontal as commonly assumed, due to the stress redistribution required for a geologically stable situation above the Veendam pillow.

Here we note that in general the present day in-situ stress state in the Northern Netherlands is not well known in the absence of measurements. This causes a significant uncertainty in subsurface integrity analyses which compute the changes in stress, starting from the initial stress. In this study (in contrast to other studies, we aimed to establish an initial stress state which is geologically stable, as a first step towards addressing this issue.

Subsidence

We computed two sets of models (**Fig. 4**): The first one (**A**) was computed to reach 52 cm subsidence (in the center of the subsidence bowl) in 31 years, and another (**B**) to 60 cm subsidence in 50 years. The subsidence bowl geometry closely resembles the results by Fokker and Visser (2014). The displacement is dominantly vertical with small horizontal components (**Fig 5**). In the layers above the Triassic, the zone of vertical motion gets wider, as expected and therefore a horizontal component of movement towards the center of the cavern field is also significant. Inside the Triassic, minor local horizontal stretching in the areas between the caverns can be observed.

Stress development

Stress changes above the cavern field show the development of two different zones (**Fig 6, 7 and 8**). Zone I is located directly above the caverns, while zone II is about 300 to 1000 m away from the caverns.

Zone I:

This zone is characterized by a drop of differential stress by up to 4.6 MPa. In the Triassic, above the caverns the decrease of differential stress ($\sigma_1 - \sigma_3$) is mostly caused by a reduction of the subvertical σ_1 principle stress (please note that the ABAQUS package uses tension as positive and in subsurface studies compression is taken as positive giving the slightly confusing color bar legend). The sub-horizontal σ_3 is also lowered in this area with smallest values in the area between caverns. Inside the Cretaceous, lower differential stress is mainly caused by an increase of the horizontal σ_3 .

Zone II:

In this zone increased differential stress values of up to 1 MPa can be observed. The increase is caused by a rise of vertical σ_1 stress in that area.

Faults in the overburden

Faults in the overburden were interpreted in the 3D seismic cube used in Raith et al., (2016), as part of a study of the risk of fault reactivation in the overburden of the Veendam Pillow. While the quality of the 3D seismic is reasonable, only the general pattern of the faults could be mapped, keeping in mind the well-known problems and limitations of fault interpretations. Results are illustrated below.

In the overburden of the Veendam Pillow two dominant fault directions are present: NE-SW striking normal faults parallel to the crest and N-S striking normal faults in NE and SW of the Veendam Pillow (**Fig. 9**). About 60 faults were mapped in the seismic images. They are up to 800m long with throw up to 150m, dipping 35-55°. The length of the faults in strike direction is about 1.5- 2 times longer than in dip direction (**Fig. 10a**).

The faults are well visible in the Cretaceous and at the top Triassic reflections. Inside the Triassic, the image rarely is good enough to allow accurate interpretation of the individual faults. None of the faults can be shown to continue to the surface, in agreement with the absence of neo-tectonic activity in the area (**Fig. 10b, 10c**).

Besides the smaller faults, two larger NE-SW striking faults parallel to the pillow's crest are present. These large faults extend from the Tertiary down to the Permian Top Salt over 1.1 km vertically with a maximal offset of about 300 m. They are up to 6 km long in strike direction. The offset of this fault is less than 150 m in the area above the caverns and is not present near the Tripscompagnie field. In the area above the active caverns, only smaller NE-SW striking faults parallel to the crest are present.

Discussion

The models presented here are a subset of many different models, which can be used to match the observed subsidence and production over time. In our models, no history match with pressure data and squeeze volumes was attempted, and our ring-shaped caverns are a simplification compared with the details of the complex connected cavern network in the subsurface, in shape and volume. On the other hand, for a more representative model the details of the geometry of the cavern network would be required. In comparison with the models of Fokker et al., 1995, we have used a more complicated cavern model, and attempted to compute a more realistic initial stress distribution in the Veendam Pillow. The initial stresses are stable over geologic time, without plasticity in the overburden, consistent with the absence of neotectonics. Based on our results, we infer (because the models match the subsidence and because the overburden is elastic), that different realizations of this model would produce similar overburden stress changes.

Considering the deformations in the overburden, in zone I it can be clearly seen that the downward movement of Top Salt above the converging cavern field leads to a decrease of vertical stresses above this area. If the caverns are close to each other the effects overlap, forming one area of decreased differential stress above them. In the shallower Cretaceous on the other hand lower differential stresses are primarily caused by horizontal shortening and therefore higher horizontal stresses. Inside zone I small increases in differential stress can only be observed directly above cavern gaps. Here horizontal stretching due to salt flow towards the caverns decreases the horizontal stress.

The subsidence above the caverns associated by a decrease in vertical stress has to be compensated outside of zone I in zone II. Here the adjacent subsidence leads to an increased vertical σ_1 resulting in slightly higher differential stresses.

In summary, cavern convergence causes vertical extension in the area above the caverns that is compensated by compression in an arc around this area (**Fig. 11**).

If we consider a Mohr Coulomb yield criterion, the stress changes in zone I produces a more stable situation than in the initial state. The stress changes in zone II on the other hand could move slightly closer to the yield criteria (shown in figure 5 by a cohesion-less 25° MC criteria for comparison). However, since these stress changes are very small, zone II can also be considered to remain stable considering that initially the area was tectonically quiet.

Conclusion

The calculated stress development shows that cavern field convergence does not change the in-situ stress to values required for fault reactivation. Therefore, no fault reactivation in the suprasalt units at the Veendam Pillow is expected. The squeeze in the salt leads to a drop of vertical stress above the caverns. Lower vertical stress leads to smaller differential stress values and therefore to more stable conditions. Further away from the caverns a slight increase of differential stress could be observed in the super salt units. However, the magnitude of this unfavorable stress development is too small to induce plastic deformation.

References

1995. *The behaviour of salt and salt caverns. Dissertation, Delft University of Technology.*
- , 2014. *Estimating the distribution of salt cavern squeeze using subsidence measurements, in: 48 Th US Rock Mechanics / Geomechanics Symposium. American Rock Mechanics Association, Minneapolis, p. ARMA 14 – 7357.*
- and (1995). *Production-induced convergence of solution mined caverns in magnesium salts and associated subsidence. In: Barends, Brouwer and Schröder (eds): Land subsidence. Natural causes, measuring techniques, the Groningen gas field. Proceedings of the fifth international conference on land subsidence, Den Haag, the Netherlands, 16-20 Oct. 1995, p. 281-289.*
- (2016) *Evolution of rheologically heterogeneous salt structures: a case study from the NE Netherlands. Solid Earth 7 (1), 67*
2005. *Microstructural evolution of deformation-modified primary halite from the Middle Triassic Röt Formation at Hengelo, The Netherlands. . 94, 941–955. doi:10.1007/s00531-005-0503-2*
1983. *Water assisted dynamic recrystallization and weakening in polycrystalline bischofite. Tectonophysics 96, 125–157. doi:10.1016/0040-1951(83)90247-0*
2008. *Flow and Transport Properties of Salt Rocks, in: Dynamics of Complex Intracontinental Basins: The Central European Basin System. pp. 277–290. doi:978-3-540-85085-4*
1981. *Creep of Bischofite, in: Proceedings, 1st Conference on the Mechanical Behaviour of Salt. Pennsylvania.*

FIGURES

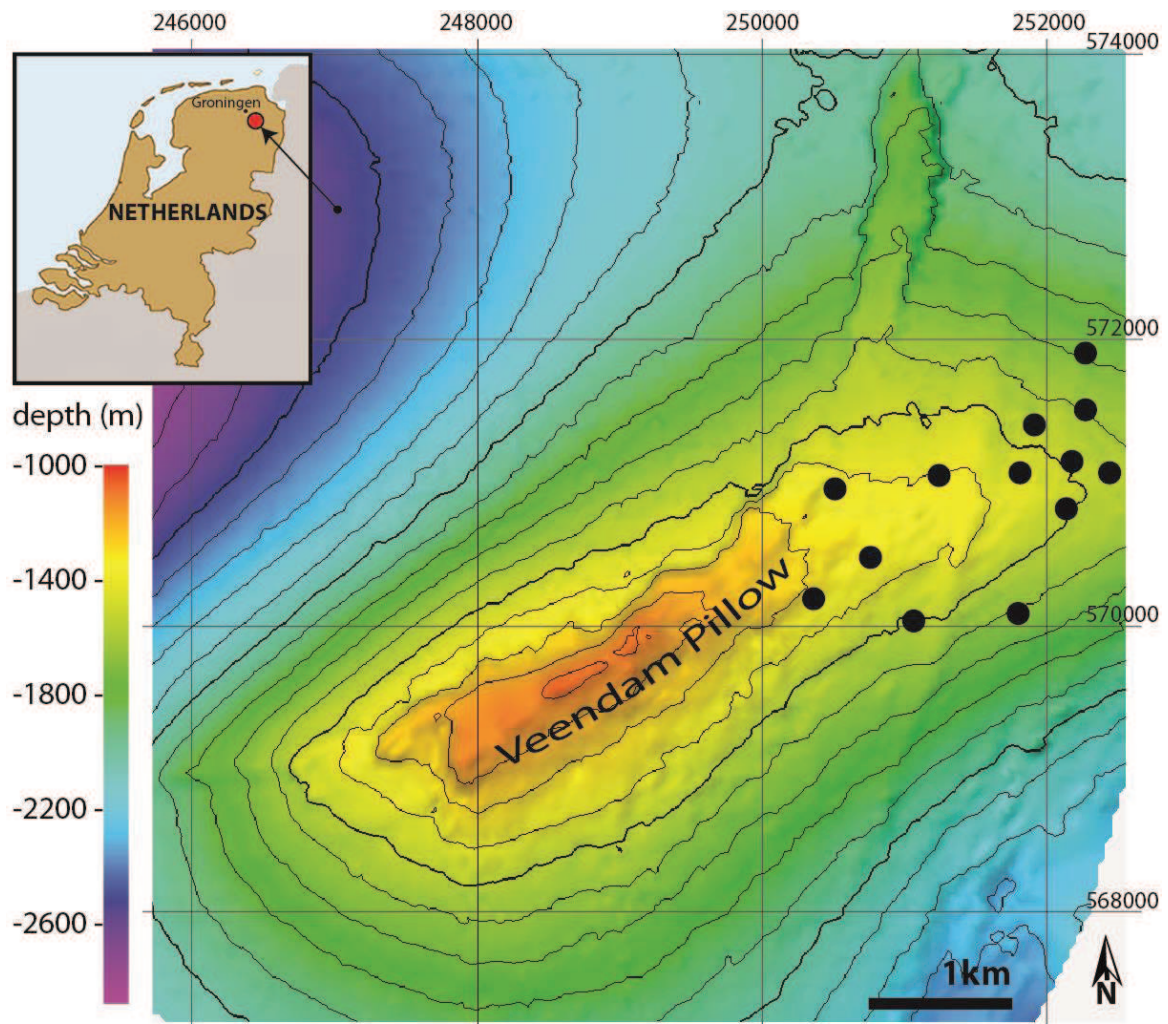


Figure 1: Depth map of top salt at the Veendam Pillow. Black points mark the position of the wells.

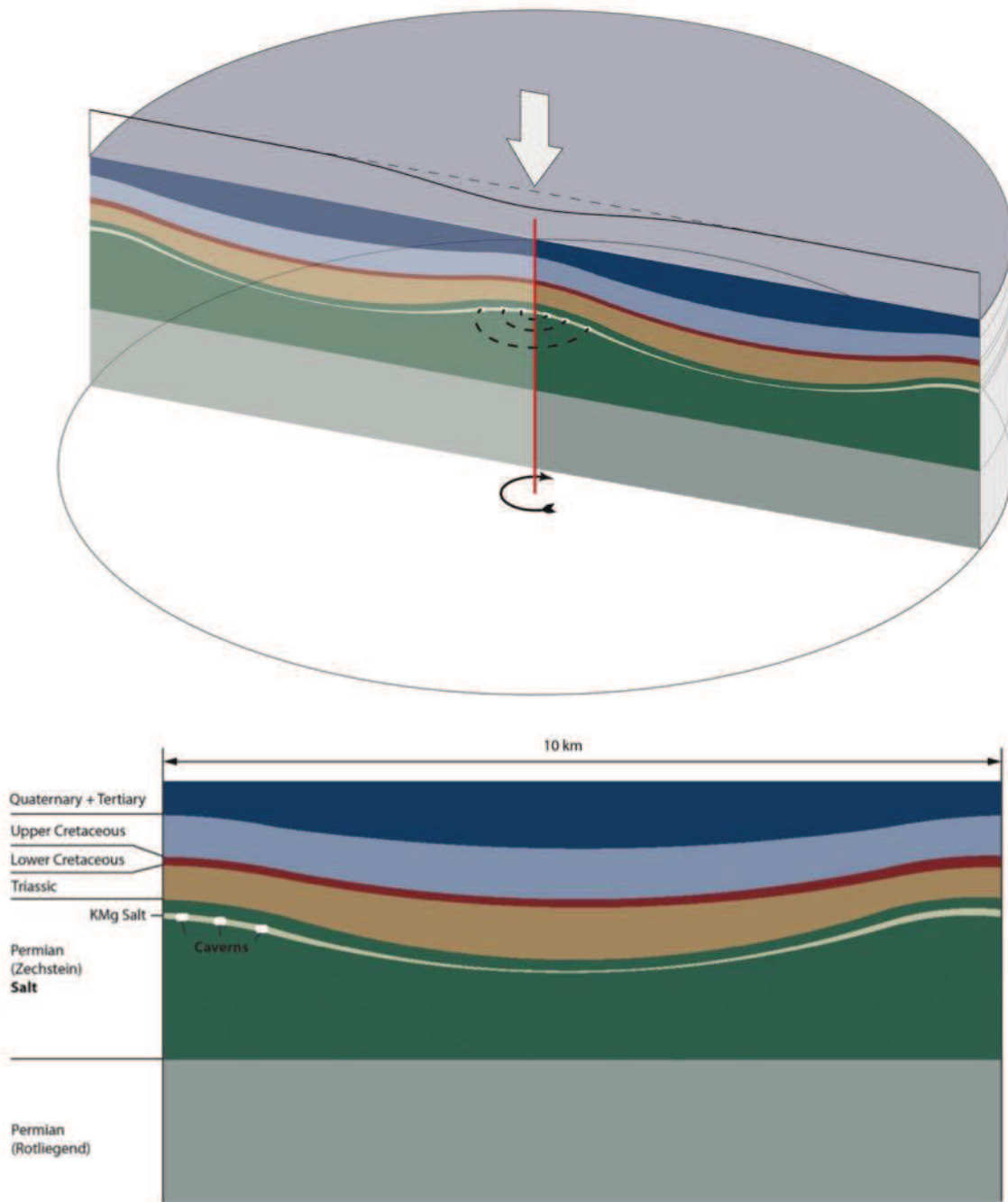


Figure 2: Geometry of the axisymmetric ABAQUS model (red line is the model center). The cavern field is modeled as three rings around the pillow center (dashed black lines).

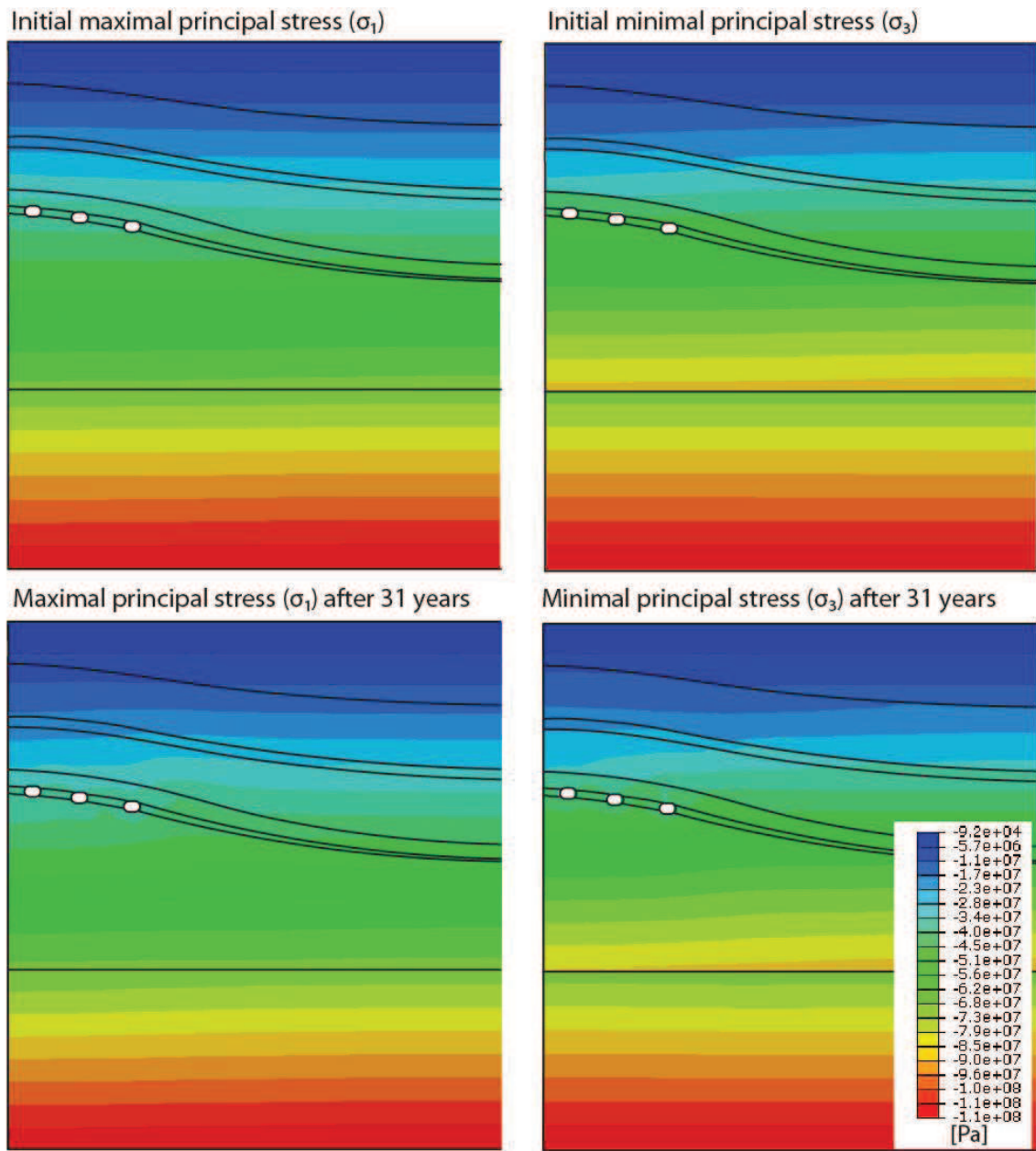


Figure 3: Maximum and minimum principle stress in the model, above: initial geologically stable situation, below: after 52 cm subsidence in 31 years. Please note that the ABAQUS package uses tension as positive and in subsurface studies compression is taken as positive giving the slightly confusing color bar legend.

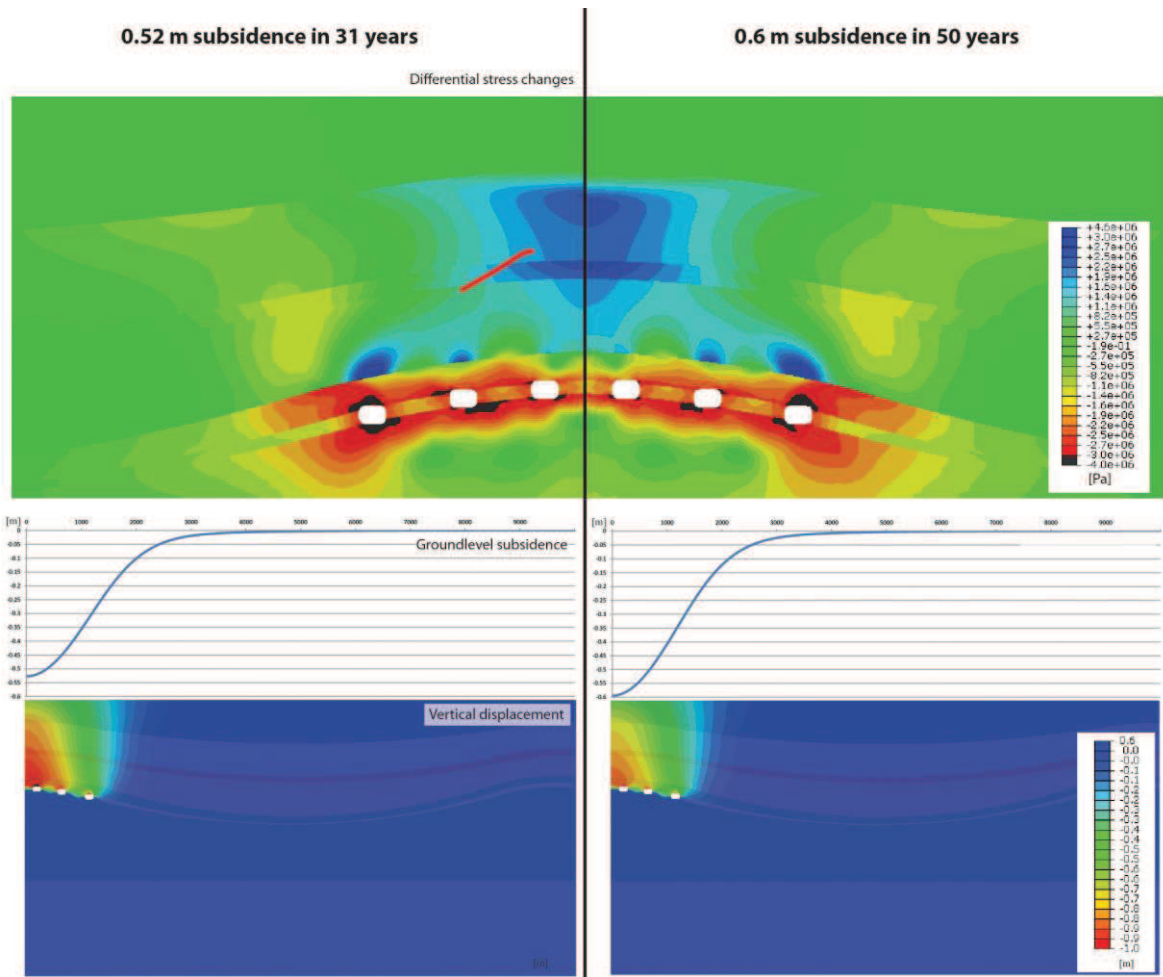


Figure 4: The two models discussed in this report. Please note that the ABAQUS package uses tension as positive and in subsurface studies compression is taken as positive giving the slightly confusing color bar legend.

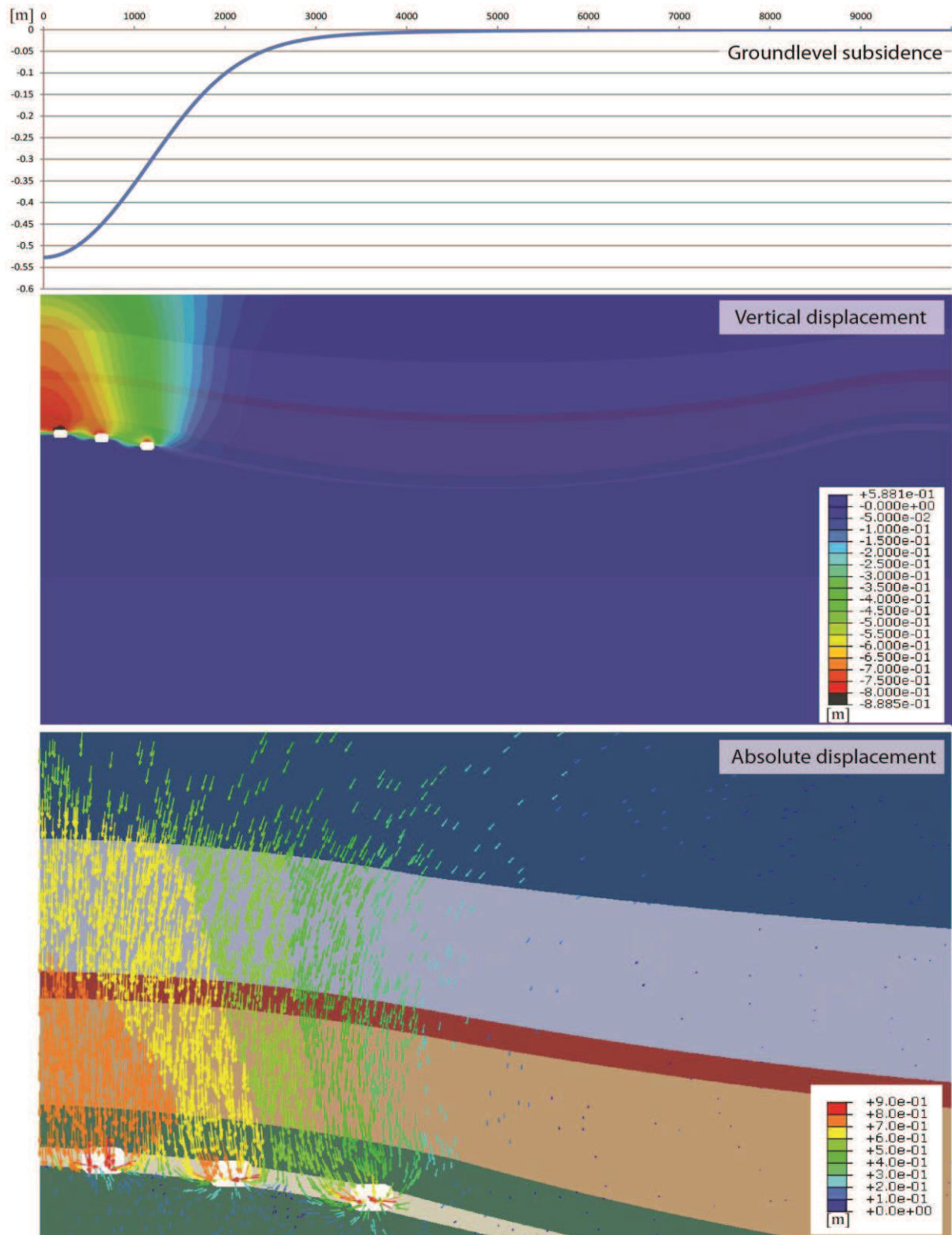


Figure 5: Displacements in the model after 1e9s (52 cm subsidence in 31 years).

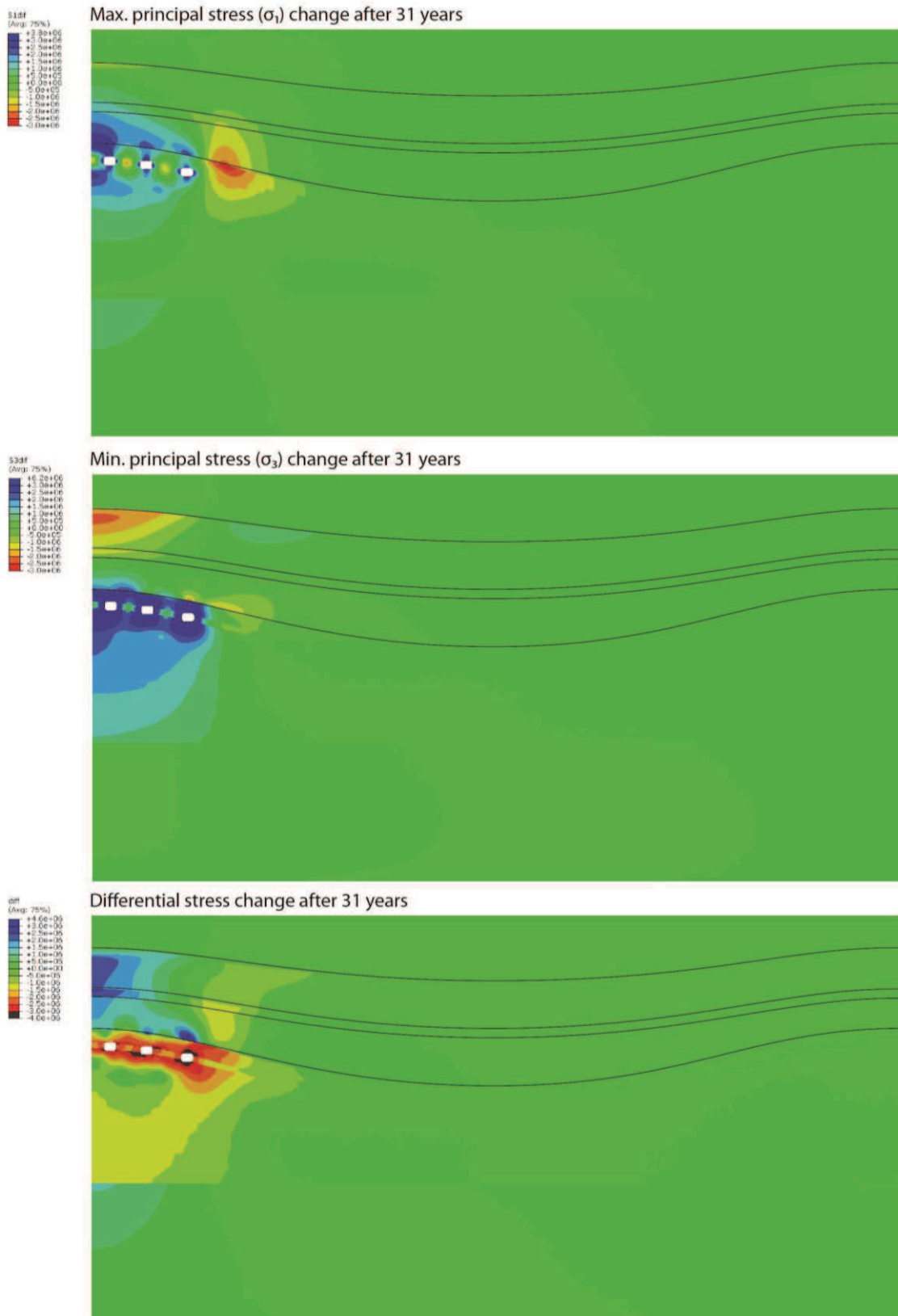


Figure 6: Development of maximum principle stress, minimum principle stress and differential stress during squeeze mining. Please note that the ABAQUS package uses tension as positive and in subsurface studies compression is taken as positive giving the slightly confusing color bar legend.

Differential stress change and deformation during the cavern shrinkage

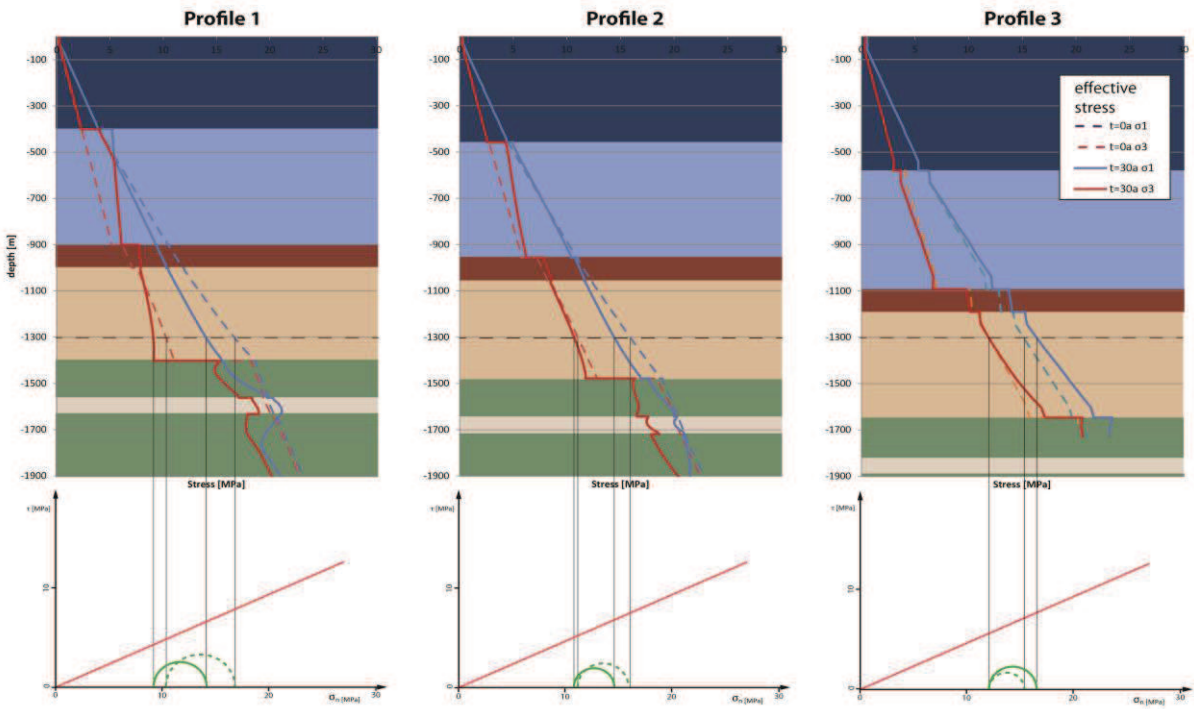
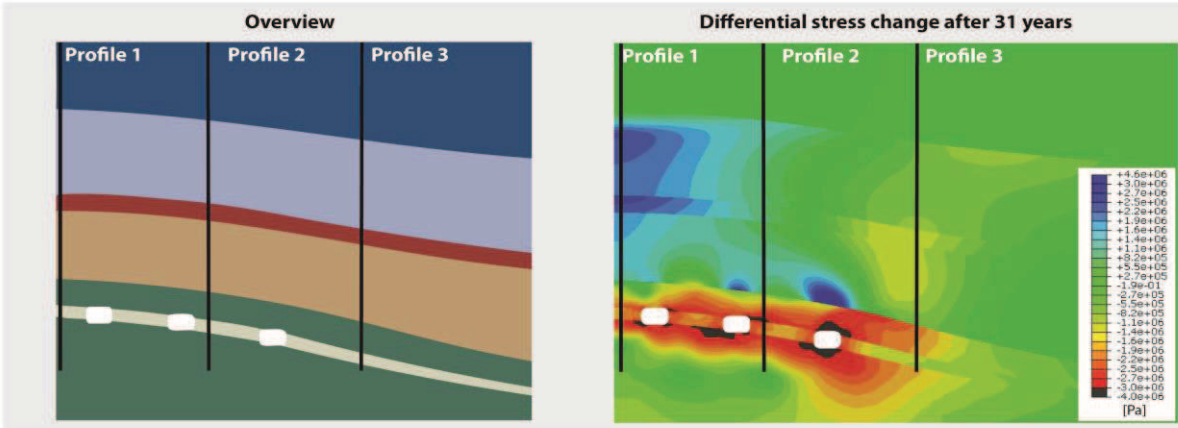
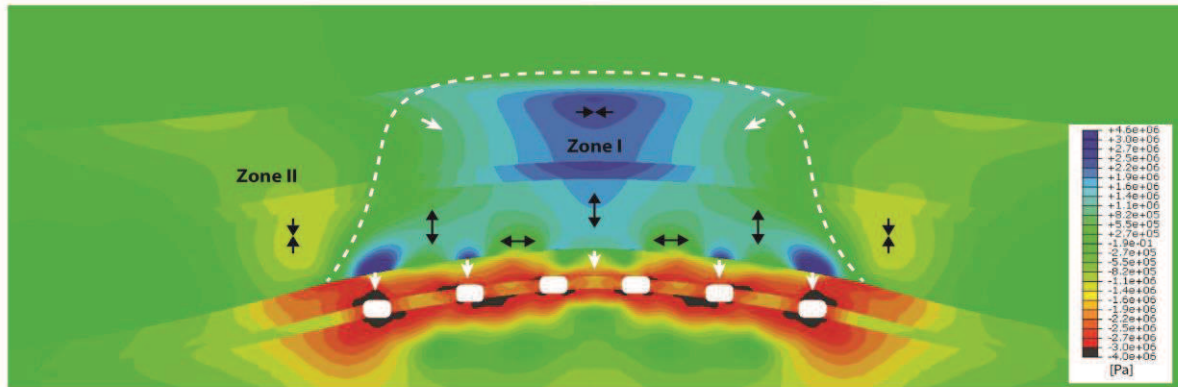


Figure 7: Model A: 52 cm subsidence in 31 years. Stress development in the overburden divided into 2 zones. The arrows indicate the relevant principle strains. (Bottom) Stress development demonstrated at three vertical stress profiles showing minimum and maximum principal stress before and after the 31 year squeeze. The Mohr-Coulomb plots show a conservative cohesionless plasticity criterion with a 25° friction angle at 1300 m depth. Please note that the ABAQUS package uses tension as positive and in subsurface studies compression is taken as positive giving the slightly confusing color bar legend.

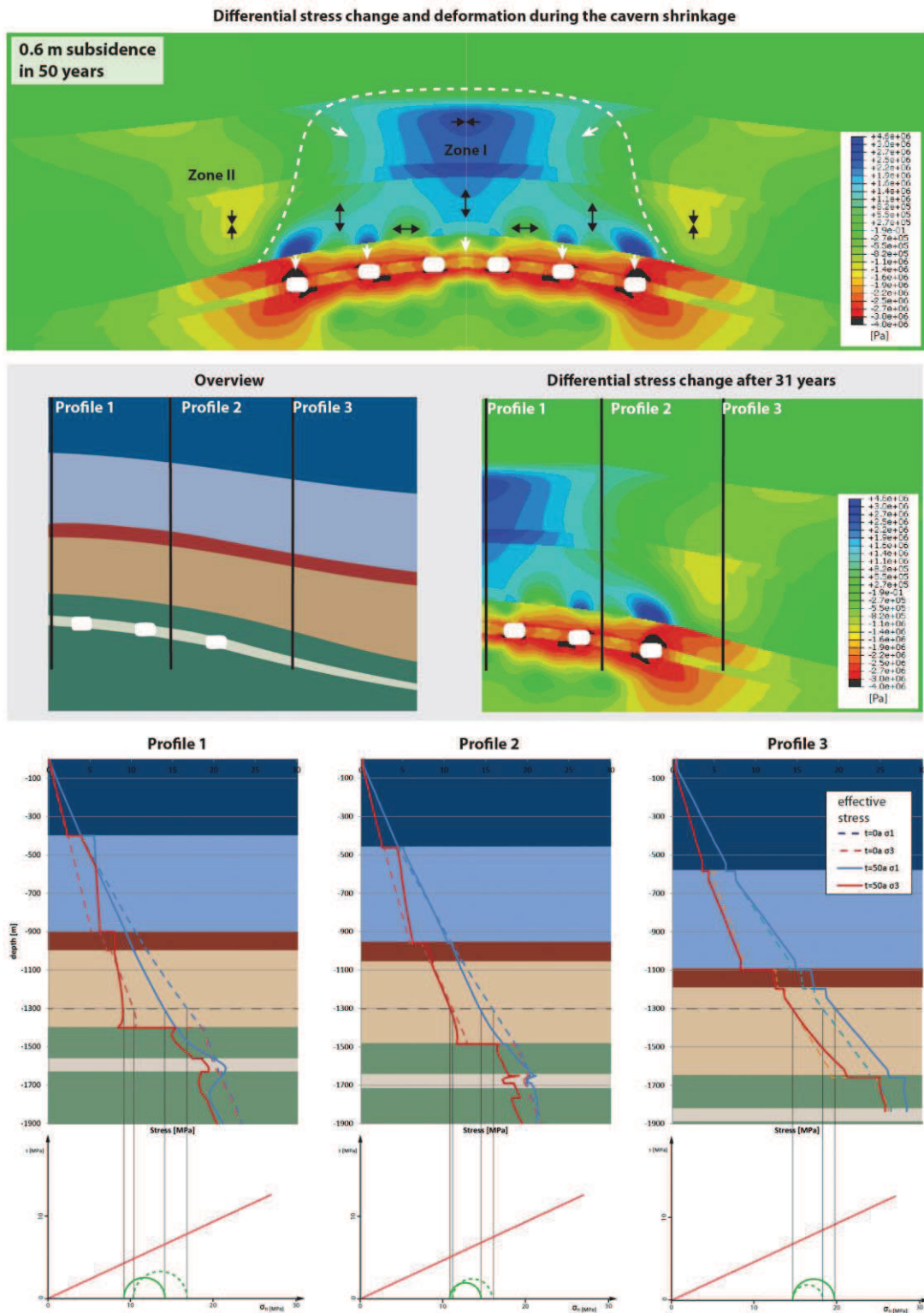


Figure 8: Model B: 60 cm subsidence in 50 years. Stress development in the overburden divided into 2 zones. The arrows indicate the relevant principle strains. (Bottom) Stress development demonstrated at three vertical stress profiles showing minimum and maximum principal stress before and after $1e9$ s. The MC plots show a conservative cohesionless plasticity criterion with a 25° friction angle at 1300 m depth. Please note that the ABAQUS package uses tension as positive and in subsurface studies compression is taken as positive giving the slightly confusing color bar legend.

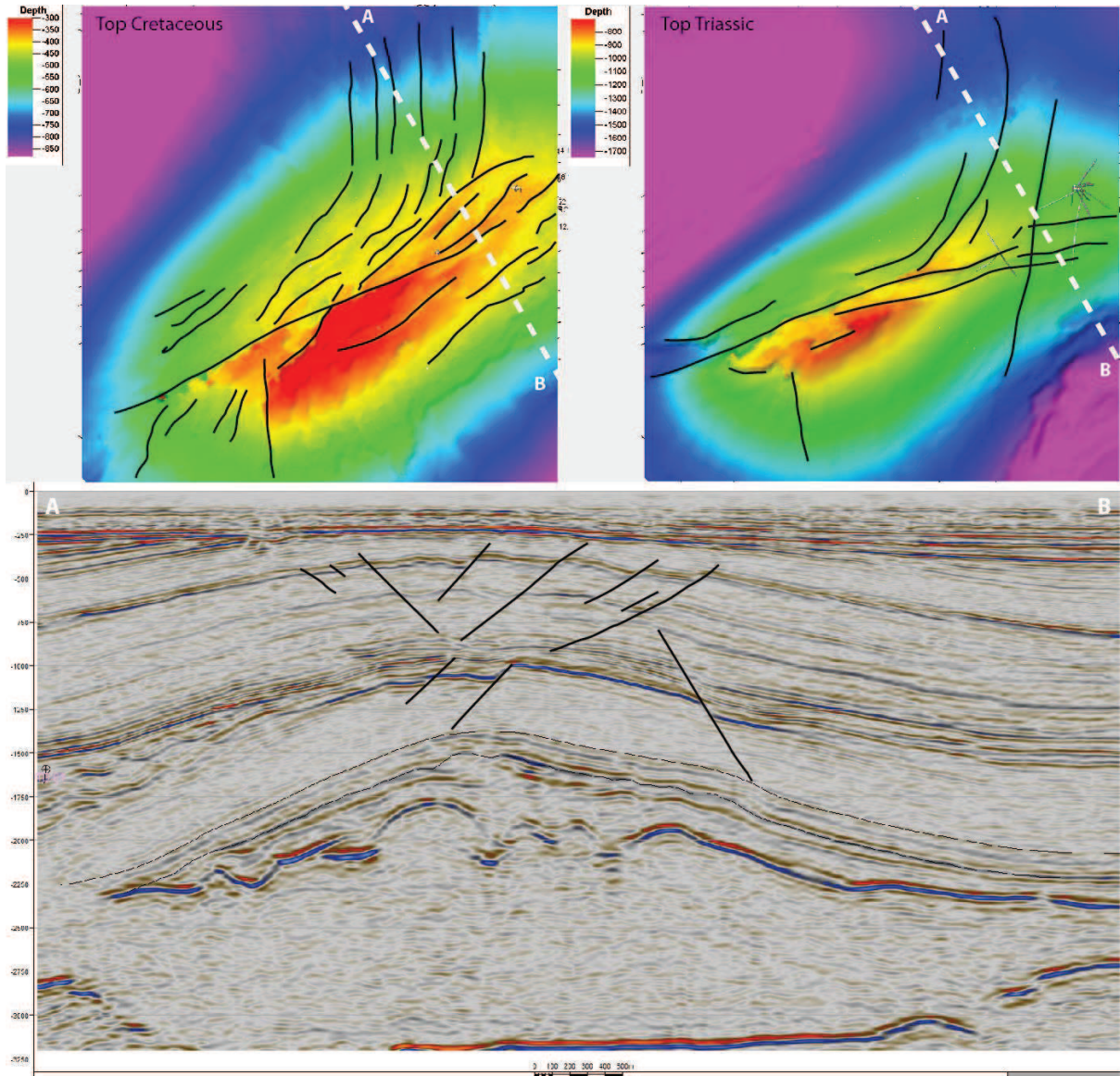


Figure 9: Top: Top Cretaceous and Top Triassic depth maps with faults indicated with black lines. Bottom: Profile A-B (vertical = horizontal scale) showing normal faults above the cavern field.

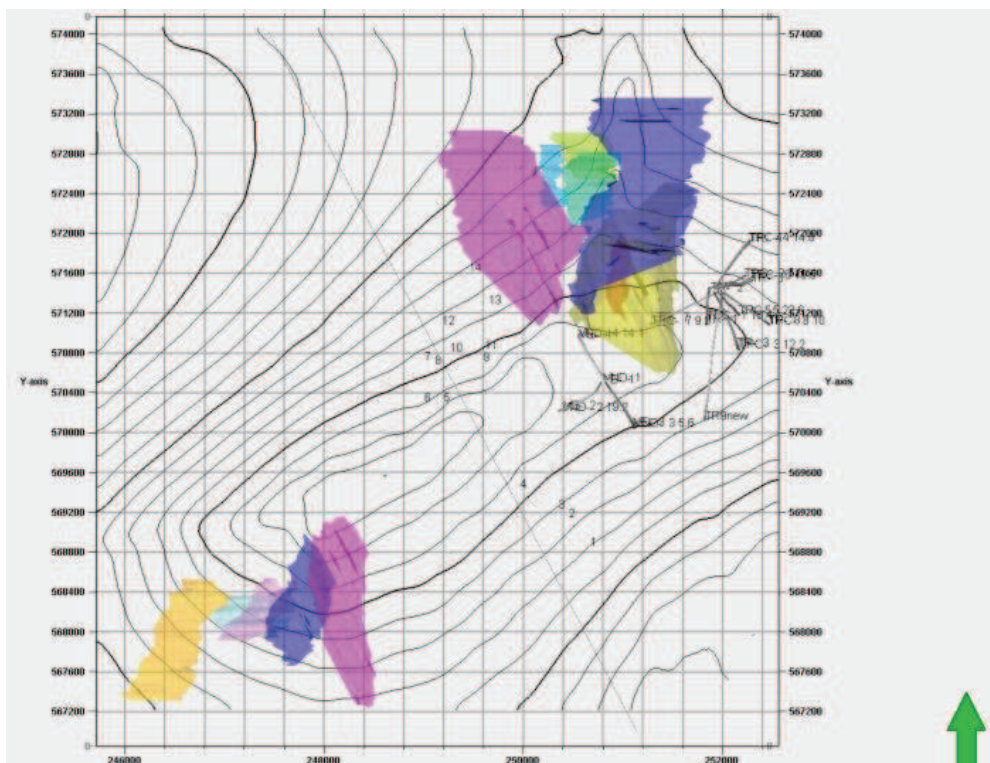
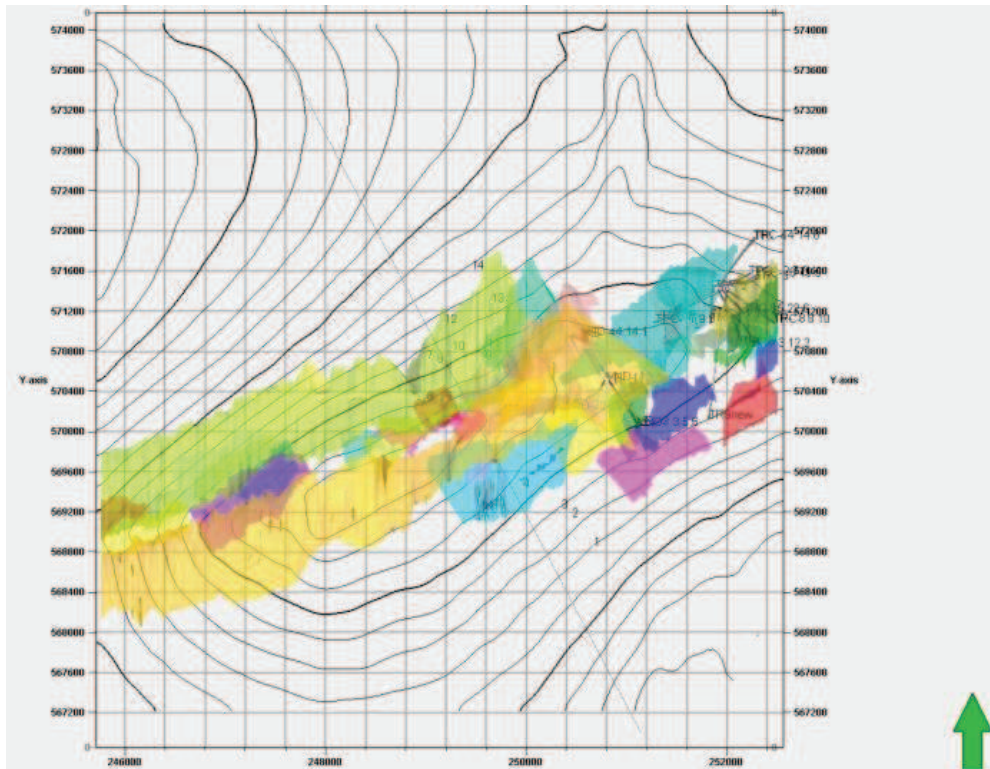


Figure 10a: Map view of N-S (upper figure) and NE-SW (lower figure) striking faults in the overburden. Each interpreted fault plane is shown by a different colour. Note that the 3D nature of these fault planes prevents better visualization in these images. The VE and TR wells are also shown. Depth of top salt is indicated by the black contour lines.

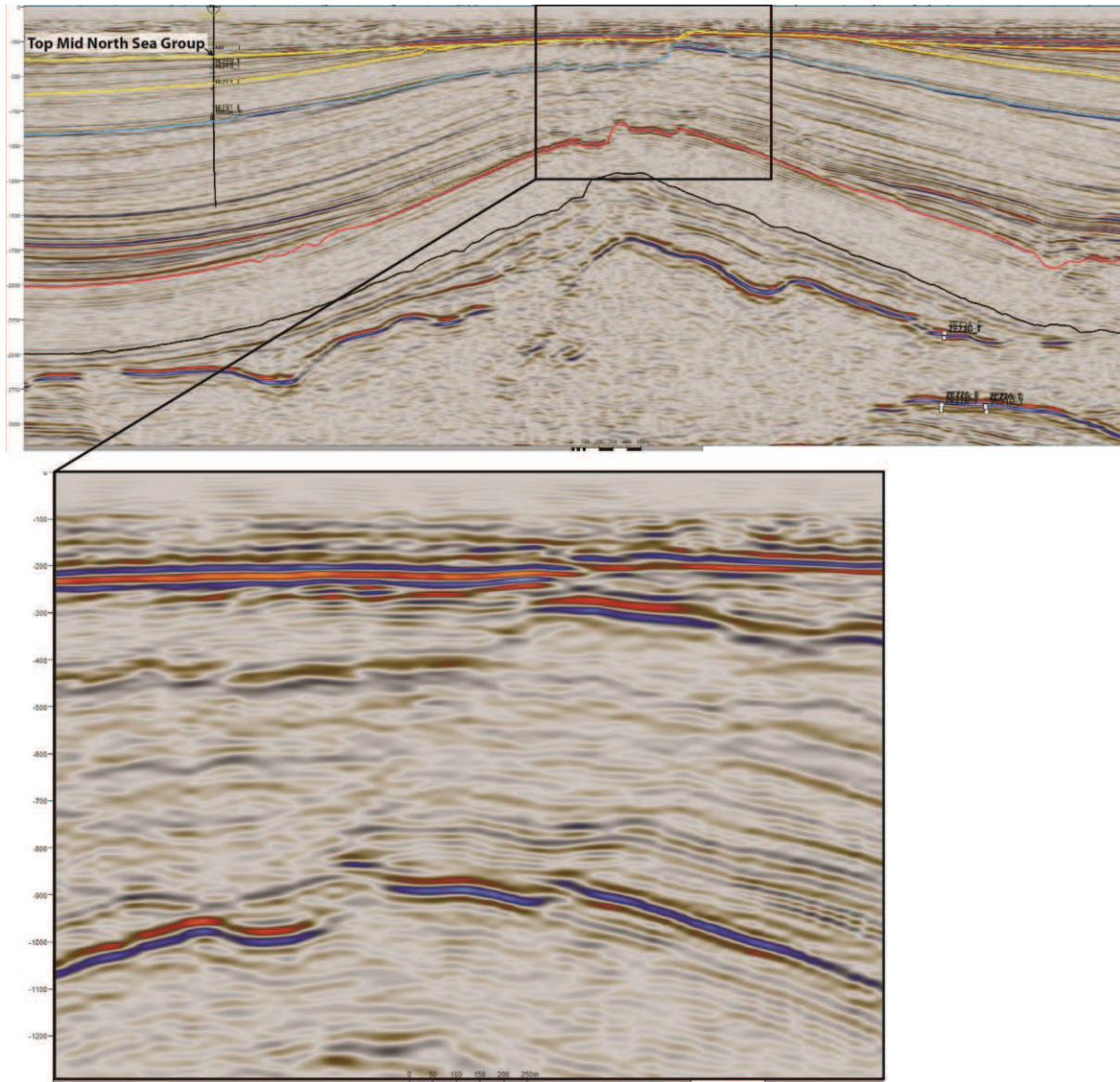
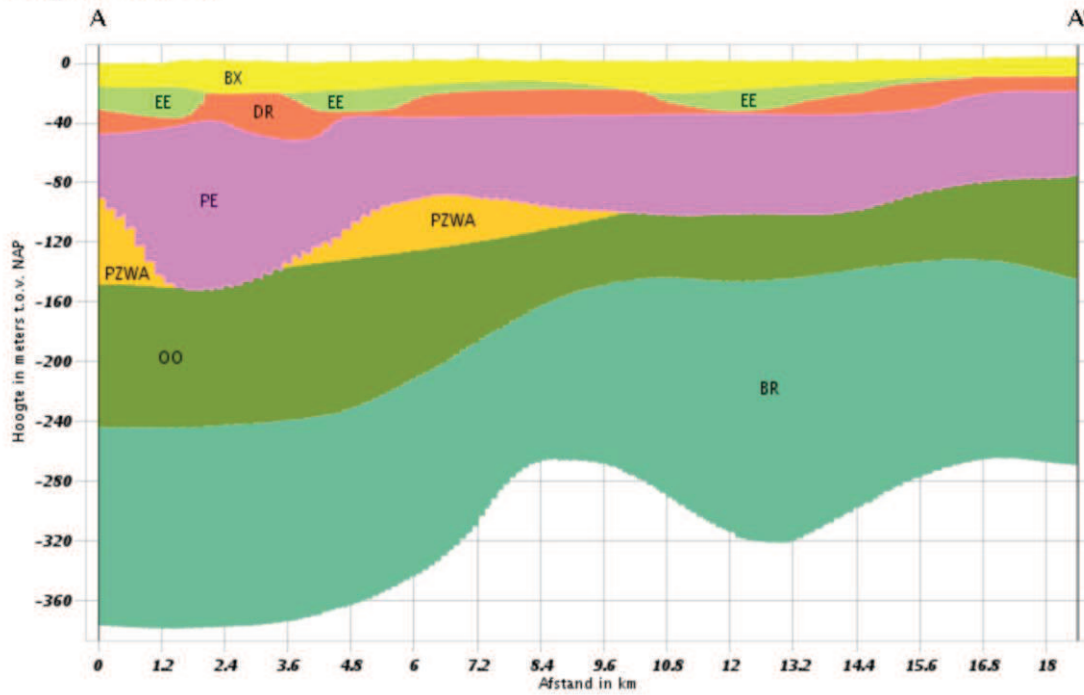


Figure 10b: NW-SE profile across the Veendam pillow, focusing on the upper part of the section. It shows the offset in the unconformity at top Mid North Sea Group, but if there is an offset in reflectors in the upper few hundred m is not clear.

Verticale Doorsnede DGM v2.2

Hoogte t.o.v. NAP: -378



Geologische eenheid

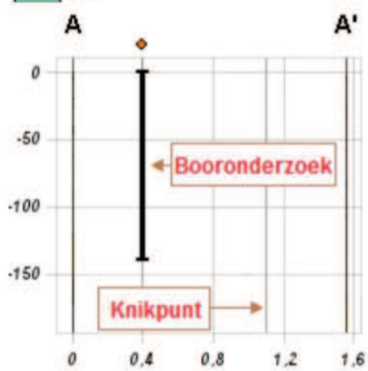


Figure 10c: NW-SE profile across the Veendam pillow, focusing on the shallow stratigraphy (from DINOLOKET). there is no growth fault apparent in the upper section.

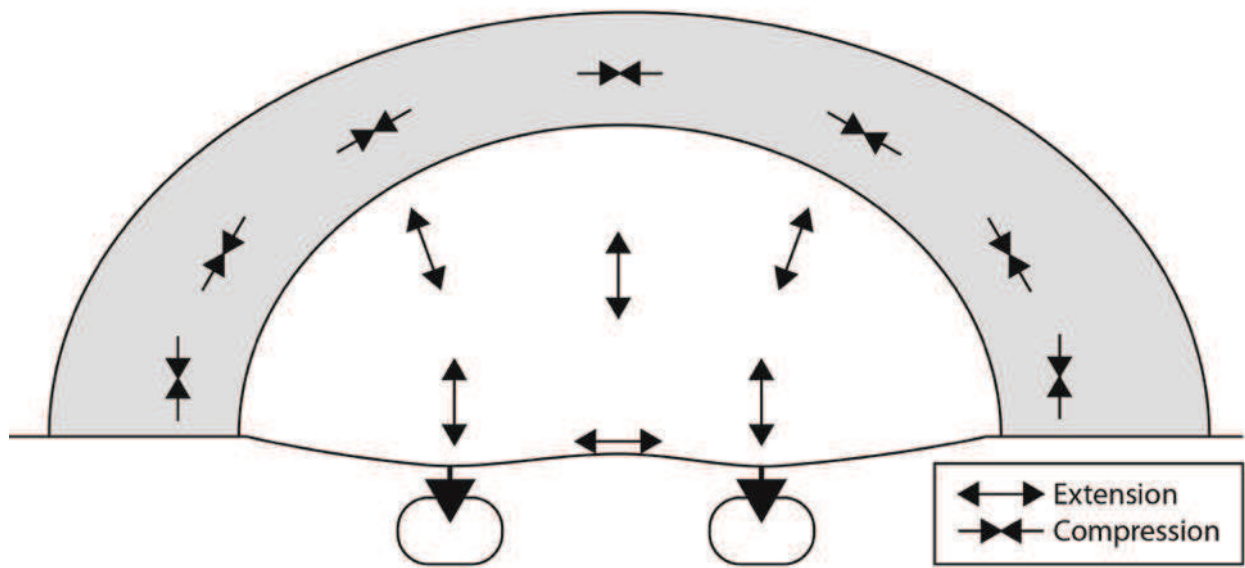


Figure 11: Simplified sketch, showing direction of relevant principle strains in the overburden.